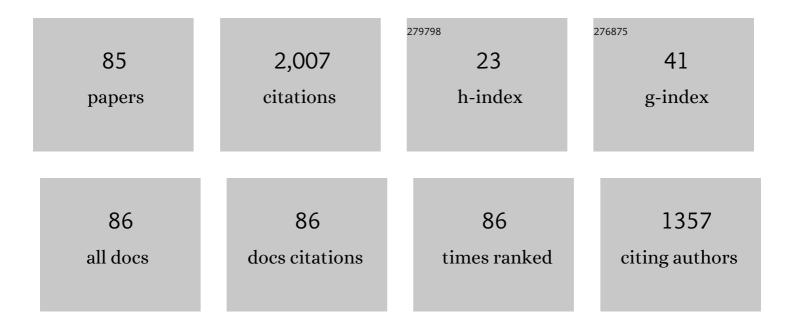
## Asuka Yamaguchi

List of Publications by Year in descending order

Source: https://exaly.com/author-pdf/7647872/publications.pdf Version: 2024-02-01



#	Article	IF	CITATIONS
1	Deformation Process and Mechanism of the Frontal Megathrust at the Nankai Subduction Zone. Geochemistry, Geophysics, Geosystems, 2022, 23, .	2.5	1
2	Constraints on Element Mobility During Deformation Within the Seismogenic Zone, Shimanto Belt, Japan. Geochemistry, Geophysics, Geosystems, 2021, 22, e2020GC009594.	2.5	5
3	Rejuvenated extension of the Philippine Sea plate and its effect on subduction dynamics in the Nankai Trough. Island Arc, 2021, 30, e12402.	1.1	6
4	Spatial Patterns in Frictional Behavior of Sediments Along the Kumano Transect in the Nankai Trough. Journal of Geophysical Research: Solid Earth, 2021, 126, .	3.4	9
5	Highly refractory dunite formation at Gibbs Island and Bruce Bank, and its role in the evolution of the circum-Antarctic continent. Canadian Mineralogist, 2021, 59, 1731-1753.	1.0	1
6	Localized fluid discharge by tensile cracking during the post-seismic period in subduction zones. Scientific Reports, 2020, 10, 12281.	3.3	3
7	Structural-morphological and sedimentary features of forearc slope off Miyagi, NE Japan: implications for development of forearc basins and plumbing systems. Geo-Marine Letters, 2020, 40, 309-324.	1.1	2
8	Deformation Structures From Splay and Décollement Faults in the Nankai Accretionary Prism, SW Japan(IODP NanTroSEIZE Expedition 316): Evidence for Slow and Rapid Slip in Fault Rocks. Geochemistry, Geophysics, Geosystems, 2020, 21, e2019GC008786.	2.5	5
9	Postseismic fluid discharge chemically recorded in altered pseudotachylyte discovered from an ancient megasplay fault: an example from the Nobeoka Thrust in the Shimanto accretionary complex, SW Japan. Progress in Earth and Planetary Science, 2019, 6, .	3.0	3
10	Origin of the early Cenozoic belt boundary thrust and Izanagi–Pacific ridge subduction in the western Pacific margin. Island Arc, 2019, 28, e12320.	1.1	31
11	Kinetic Models for Healing of the Subduction Interface Based on Observations of Ancient Accretionary Complexes. Geochemistry, Geophysics, Geosystems, 2019, 20, 3431-3449.	2.5	17
12	Fluorine and chlorine fractionation during magma ocean crystallization: Constraints on the origin of the non-chondritic F/Cl ratio of the Earth. Earth and Planetary Science Letters, 2019, 520, 241-249.	4.4	5
13	Monsoon-influenced variations in plankton community structure and upper-water column stratification in the western Bay of Bengal during the past 80†ky. Palaeogeography, Palaeoclimatology, Palaeoecology, 2019, 521, 138-150.	2.3	11
14	Distributed deformation along the subduction plate interface: The role of tectonic mélanges. Lithos, 2019, 334-335, 69-87.	1.4	15
15	Evaluation from otolith Sr stable isotope ratios of possible juvenile growth areas of Japanese eels collected from the West Mariana Ridge spawning area. Fisheries Science, 2019, 85, 483-493.	1.6	7
16	Indian Monsoonal Variations During the Past 80ÂKyr Recorded in NGHPâ€02 Hole 19B, Western Bay of Bengal: Implications From Chemical and Mineral Properties. Geochemistry, Geophysics, Geosystems, 2019, 20, 148-165.	2.5	12
17	Evidence for surface sediment remobilization by earthquakes in the Nankai forearc region from sedimentary records. Geological Society Special Publication, 2019, 477, 37-45.	1.3	9
18	Threeâ€dimensional texture of natural pseudotachylyte: Pseudotachylyte formation mechanism in hydrous accretionary complex. Island Arc, 2018, 27, e12241.	1.1	0

Аѕика Үамадисні

#	Article	IF	CITATIONS
19	Spatial variability in sediment lithology and sedimentary processes along the Japan Trench: use of deep-sea turbidite records to reconstruct past large earthquakes. Geological Society Special Publication, 2018, 456, 75-89.	1.3	28
20	Fluid properties and dynamics along the seismogenic plate interface. , 2018, 14, 469-491.		20
21	New geochemical data for back-arc basin basalts from DSDP Leg 58 Sites 442-444 and the ODP Leg 131 Site 808, Shikoku Basin. Journal of the Geological Society of Japan, 2018, 124, 935-940.	0.6	0
22	Dynamic formation process of thick deformation zone on the shallow plate boundary fault of the Japan Trench: insight from analog experiments of half-graben subduction. Progress in Earth and Planetary Science, 2018, 5, .	3.0	4
23	Acoustic properties of deformed rocks in the <scp>N</scp> obeoka thrust, in the <scp>S</scp> himanto <scp>B</scp> elt, <scp>K</scp> yushu, <scp>S</scp> outhwest <scp>J</scp> apan. Island Arc, 2017, 26, e12198.	1.1	1
24	Tertiary evolution of the Shimanto belt (Japan): A largeâ€scale collision in Early Miocene. Tectonics, 2017, 36, 1317-1337.	2.8	16
25	Organic matter cracking: A source of fluid overpressure in subducting sediments. Tectonophysics, 2017, 721, 254-274.	2.2	17
26	Stress State in the Kumano Basin and in Slope Sediment Determined From Anelastic Strain Recovery: Results From IODP Expedition 338 to the Nankai Trough. Geochemistry, Geophysics, Geosystems, 2017, 18, 3608-3616.	2.5	7
27	High Pressure Experiments on Metalâ€5ilicate Partitioning of Chlorine in a Magma Ocean: Implications for Terrestrial Chlorine Depletion. Geochemistry, Geophysics, Geosystems, 2017, 18, 3929-3945.	2.5	8
28	Temporal stress variations along a seismogenic megasplay fault in the subduction zone: <scp>A</scp> n example from the <scp>N</scp> obeoka <scp>T</scp> hrust, southwestern <scp>J</scp> apan. Island Arc, 2017, 26, e12193.	1.1	5
29	Alteration and dehydration of subducting oceanic crust within subduction zones: implications for décollement step-down and plate-boundary seismogenesis. Earth, Planets and Space, 2017, 69, .	2.5	14
30	Opalâ€CT in chert beneath the toe of the Tohoku margin and its influence on the seismic aseismic transition in subduction zones. Geophysical Research Letters, 2017, 44, 687-693.	4.0	2
31	Paleothermal structure of the <scp>N</scp> ankai inner accretionary wedge estimated from vitrinite reflectance of cuttings. Geochemistry, Geophysics, Geosystems, 2017, 18, 3185-3196.	2.5	11
32	Source and sink of fluid in pelagic siliceous sediments along a cold subduction plate boundary. Tectonophysics, 2016, 686, 146-157.	2.2	2
33	Variations in stress and driving pore fluid pressure ratio using vein orientations along megasplay faults : Example from the Nobeoka Thrust, Southwest Japan. Island Arc, 2016, 25, 421-432.	1.1	10
34	Deformation processes at the down-dip limit of the seismogenic zone: The example of Shimanto accretionary complex. Tectonophysics, 2016, 687, 28-43.	2.2	23
35	UAVâ€based mesoscale lithologic distribution map of a large shear zone in Jurassic accretionary complex (Ohwaki outcrop in the Mino Belt, central Japan). Island Arc, 2016, 25, 436-438.	1.1	1
36	Hydrogeological responses to incoming materials at the erosional subduction margin, offshore <scp>O</scp> sa <scp>P</scp> eninsula, <scp>C</scp> osta <scp>R</scp> ica. Geochemistry, Geophysics, Geosystems, 2015, 16, 2725-2742.	2.5	11

Аѕика Үамадисні

#	Article	IF	CITATIONS
37	Lithification facilitates frictional instability in argillaceous subduction zone sediments. Tectonophysics, 2015, 665, 177-185.	2.2	16
38	Possible mechanism of mud volcanism at the prism-backstop contact in the western Mediterranean Ridge Accretionary Complex. Marine Geology, 2015, 363, 52-64.	2.1	11
39	Fluid circulation in the depths of accretionary prisms: an example of the Shimanto Belt, Kyushu, Japan. Tectonophysics, 2015, 655, 161-176.	2.2	25
40	Multiple damage zone structure of an exhumed seismogenic megasplay fault in a subduction zone - a study from the Nobeoka Thrust Drilling Project. Earth, Planets and Space, 2015, 67, .	2.5	15
41	Estimation of slip rate and fault displacement during shallow earthquake rupture in the Nankai subduction zone. Earth, Planets and Space, 2015, 67, .	2.5	15
42	Fluid-rock interaction recorded in black fault rocks in the Kodiak accretionary complex, Alaska. Earth, Planets and Space, 2014, 66, .	2.5	11
43	Friction properties of the plate boundary megathrust beneath the frontal wedge near the Japan Trench: an inference from topographic variation. Earth, Planets and Space, 2014, 66, .	2.5	19
44	Stress reversal recorded in calcite vein cuttings from the Nankai accretionary prism, southwest Japan. Earth, Planets and Space, 2014, 66, .	2.5	7
45	Changes in illite crystallinity within an ancient tectonic boundary thrust caused by thermal, mechanical, and hydrothermal effects: an example from the Nobeoka Thrust, southwest Japan. Earth, Planets and Space, 2014, 66, 116.	2.5	25
46	Quartz deposition and its influence on the deformation process of megathrusts in subduction zones. Earth, Planets and Space, 2014, 66, .	2.5	7
47	Middle Miocene swift migration of the TTT triple junction and rapid crustal growth in southwest Japan: A review. Tectonics, 2014, 33, 1219-1238.	2.8	104
48	A new method of reconstituting the P–T conditions of fluid circulation in an accretionary prism (Shimanto, Japan) from microthermometry of methane-bearing aqueous inclusions. Geochimica Et Cosmochimica Acta, 2014, 125, 96-109.	3.9	20
49	Long-term evolution of an accretionary prism: The case study of the Shimanto Belt, Kyushu, Japan. Tectonics, 2014, 33, 936-959.	2.8	42
50	The influence of organic–rich shear zones on pelagic sediment deformation and seismogenesis in a subduction zone. Journal of Mineralogical and Petrological Sciences, 2014, 109, 228-238.	0.9	2
51	Hanging wall deformation of a seismogenic megasplay fault in an accretionary prism: The Nobeoka Thrust in southwestern Japan. Journal of Structural Geology, 2013, 52, 136-147.	2.3	25
52	Contrasts in physical properties between the hanging wall and footwall of an exhumed seismogenic megasplay fault in a subduction zone—An example from the Nobeoka Thrust Drilling Project. Geochemistry, Geophysics, Geosystems, 2013, 14, 5354-5370.	2.5	22
53	Unconformity between a <scp>L</scp> ate <scp>M</scp> iocene– <scp>P</scp> liocene accretionary prism ( <scp>N</scp> ishizaki <scp>F</scp> ormation) and <scp>P</scp> liocene trenchâ€slope sediments ( <scp>K</scp> agamigaura <scp>F</scp> ormation), central <scp>J</scp> apan. Island Arc, 2012, 21, 231-234.	1.1	5
54	Tectonic mélange as fault rock of subduction plate boundary. Tectonophysics, 2012, 568-569, 25-38.	2.2	97

#	Article	IF	CITATIONS
55	Silica diagenesis and its effect on interplate seismicity in cold subduction zones. Earth and Planetary Science Letters, 2012, 317-318, 136-144.	4.4	22
56	Runaway slip to the trench due to rupture of highly pressurized megathrust beneath the middle trench slope: The tsunamigenesis of the 2011 Tohoku earthquake off the east coast of northern Japan. Earth and Planetary Science Letters, 2012, 339-340, 32-45.	4.4	81
57	Sources and physicochemical characteristics of fluids along a subductionâ€zone megathrust: A geochemical approach using synâ€ŧectonic mineral veins in the Mugi mélange, Shimanto accretionary complex. Geochemistry, Geophysics, Geosystems, 2012, 13, .	2.5	39
58	A new source of water in seismogenic subduction zones. Geophysical Research Letters, 2011, 38, n/a-n/a.	4.0	34
59	Dynamic changes in fluid redox state associated with episodic fault rupture along a megasplay fault in a subduction zone. Earth and Planetary Science Letters, 2011, 302, 369-377.	4.4	54
60	Smectite to chlorite conversion by frictional heating along a subduction thrust. Earth and Planetary Science Letters, 2011, 305, 161-170.	4.4	41
61	Progressive illitization in fault gouge caused by seismic slip propagation along a megasplay fault in the Nankai Trough. Geology, 2011, 39, 995-998.	4.4	59
62	Seismic slip propagation to the updip end of plate boundary subduction interface faults: Vitrinite reflectance geothermometry on Integrated Ocean Drilling Program NanTro SEIZE cores. Geology, 2011, 39, 395-398.	4.4	147
63	Record of mega-earthquakes in subduction thrusts: The black fault rocks of Pasagshak Point (Kodiak) Tj ETQq1	. 1 0. <u>78</u> 431	4 rggT /Over
64	Geological record of thermal pressurization and earthquake instability of subduction thrusts. Tectonophysics, 2010, 485, 260-268.	2.2	14
65	Interactions between deformation and fluids in the frontal thrust region of the NanTroSEIZE transect offshore the Kii Peninsula, Japan: Results from IODP Expedition 316 Sites C0006 and C0007. Geochemistry, Geophysics, Geosystems, 2009, 10, .	2.5	65
66	Anelastic strain recovery reveals extension across SW Japan subduction zone. Geophysical Research Letters, 2009, 36, .	4.0	75
67	Structural architecture and active deformation of the Nankai Accretionary Prism, Japan: Submersible survey results from the Tenryu Submarine Canyon. Bulletin of the Geological Society of America, 2009, 121, 1629-1646.	3.3	52
68	Deformation and fluid flow in seismogenic subduction zone: The Mugi Mélange in the Shimanto Belt. Journal of the Geological Society of Japan, 2009, 115, S21-S36.	0.6	2
69	Stretching of fluid inclusions in calcite as an indicator of frictional heating on faults. Geology, 2008, 36, 111.	4.4	40
70	Links among mountain building, surface erosion, and growth of an accretionary prism in a subduction zone—An example from southwest Japan. , 2008, , 391-403.		6
71	Transition of accretionary wedge structures around the up-dip limit of the seismogenic subduction zone. Earth and Planetary Science Letters, 2007, 255, 471-484.	4.4	116
72	Fluidization of granular material in a subduction thrust at seismogenic depths. Earth and Planetary Science Letters, 2007, 259, 307-318.	4.4	83

Аѕика Үамадисні

#	Article	IF	CITATIONS
73	Fluid Behavior during Evolution of Plate Boundary Fault from Trench to Seismogenic Depths. Journal of Geography (Chigaku Zasshi), 2006, 115, 353-366.	0.3	3
74	Tectonic incorporation of the upper part of oceanic crust to overriding plate of a convergent margin: An example from the Cretaceous–early Tertiary Mugi Mélange, the Shimanto Belt, Japan. Tectonophysics, 2005, 401, 217-230.	2.2	76
75	Deformation and fluid flow of a major out-of-sequence thrust located at seismogenic depth in an accretionary complex: Nobeoka Thrust in the Shimanto Belt, Kyushu, Japan. Tectonics, 2005, 24, n/a-n/a.	2.8	79
76	Cretaceous–Neogene accretionary units. , 0, , 125-137.		3
77	Site C0002. Proceedings of the Integrated Ocean Drilling Program Integrated Ocean Drilling Program, 0, , .	1.0	32
78	Site C0018. Proceedings of the Integrated Ocean Drilling Program Integrated Ocean Drilling Program, 0, , .	1.0	5
79	Site C0021. Proceedings of the Integrated Ocean Drilling Program Integrated Ocean Drilling Program, 0, , .	1.0	7
80	Generation Depth of the Pseudotachylyte from an Out-of-Sequence Thrust in Accretionary Prism – Geothermobarometric Evidence. Scientific Drilling, 0, SpecialIssue, 47-50.	0.6	9
81	Site C0022. Proceedings of the Integrated Ocean Drilling Program Integrated Ocean Drilling Program, 0, , .	1.0	5
82	Site C0002. Proceedings of the International Ocean Discovery Program, 0, , .	0.0	6
83	Site C0025. Proceedings of the International Ocean Discovery Program, 0, , .	0.0	2
84	Site C0024. Proceedings of the International Ocean Discovery Program, 0, , .	0.0	1
85	Upper-plate tectonic hysteresis and segmentation of the rupture area during seismogenesis in subduction zones—A case study of the Nankai Trough. , 0, , .		0